

Stress analysis and tests on a one-sheet hyperboloidal tower

Autor(en): **Kato, Ben**

Objektyp: **Article**

Zeitschrift: **IABSE congress report = Rapport du congrès AIPC = IVBH
Kongressbericht**

Band (Jahr): **7 (1964)**

PDF erstellt am: **13.09.2024**

Persistenter Link: <https://doi.org/10.5169/seals-7844>

Nutzungsbedingungen

Die ETH-Bibliothek ist Anbieterin der digitalisierten Zeitschriften. Sie besitzt keine Urheberrechte an den Inhalten der Zeitschriften. Die Rechte liegen in der Regel bei den Herausgebern.

Die auf der Plattform e-periodica veröffentlichten Dokumente stehen für nicht-kommerzielle Zwecke in Lehre und Forschung sowie für die private Nutzung frei zur Verfügung. Einzelne Dateien oder Ausdrucke aus diesem Angebot können zusammen mit diesen Nutzungsbedingungen und den korrekten Herkunftsbezeichnungen weitergegeben werden.

Das Veröffentlichen von Bildern in Print- und Online-Publikationen ist nur mit vorheriger Genehmigung der Rechteinhaber erlaubt. Die systematische Speicherung von Teilen des elektronischen Angebots auf anderen Servern bedarf ebenfalls des schriftlichen Einverständnisses der Rechteinhaber.

Haftungsausschluss

Alle Angaben erfolgen ohne Gewähr für Vollständigkeit oder Richtigkeit. Es wird keine Haftung übernommen für Schäden durch die Verwendung von Informationen aus diesem Online-Angebot oder durch das Fehlen von Informationen. Dies gilt auch für Inhalte Dritter, die über dieses Angebot zugänglich sind.

Stress Analysis and Tests on a One-sheet Hyperboloidal Tower

Calcul des contraintes et essais sur une tour en hyperboloïde à une nappe
Spannungsanalyse und Versuche an einem einschaligen Hyperboloid-Turm

BEN KATO

Assistant Professor, University of Tokyo

1. Introduction

A one-sheet hyperboloidal tower, as shown in Fig. 1, is now under construction on the 3rd pier of the port of *Kobe*. This tower consists of an outer net of one-sheet hyperboloid and the elevator shaft located in the core; diaphragms between the net and the shaft are distributed at each node level of the net ($a \dots f$ in fig. 2). The members of the net are made of high tensile steel tubes, and they are connected by high-strength bolts at every node.

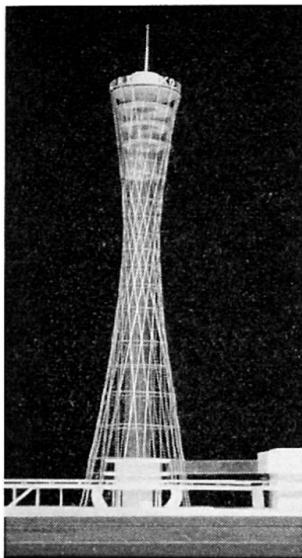


Fig. 1.

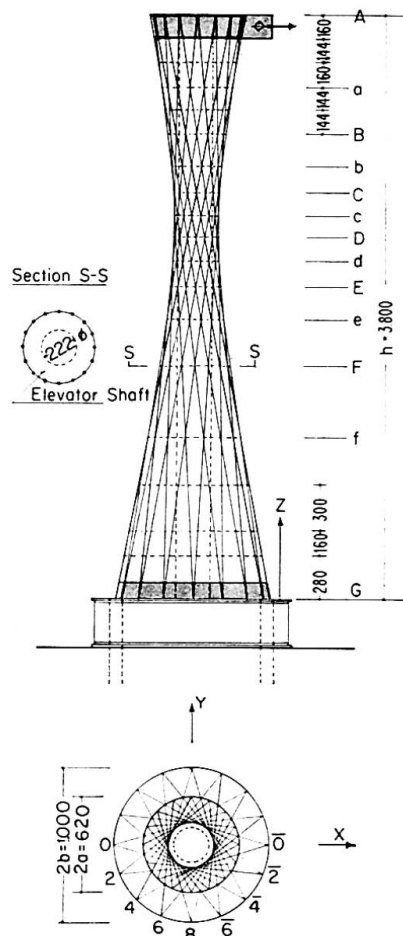


Fig. 2.

In this paper the stress calculation and the results of model tests on this structure, when subjected to lateral forces such as the seismic load, are discussed.

2. Geometrical Properties of the Hyperboloid

- a) The net consists of sixteen pairs of family generators as shown in Fig. 2, and one of them is

$$\frac{z}{h} = \frac{x + \frac{b}{\sqrt{2}}}{a + \frac{b}{\sqrt{2}}} = \frac{y + \frac{b}{\sqrt{2}}}{\frac{b}{\sqrt{2}}}, \quad \frac{x + \frac{b}{\sqrt{2}}}{a + \frac{b}{\sqrt{2}}} = \frac{y - \frac{b}{\sqrt{2}}}{-\frac{b}{\sqrt{2}}} = \frac{z}{h}. \quad (1)$$

Enveloping these generators, we have an equation of one-sheet hyperboloid

$$r^2 = x^2 + y^2 = \left\{ \frac{z}{h} \left(\frac{a}{\sqrt{2}} + b \right) - b \right\}^2 + \left(\frac{z}{h} \frac{a}{\sqrt{2}} \right)^2. \quad (2)$$

- b) The Z -co-ordinate of each node $a \sim f$ may be calculated as that of the point of intersection of corresponding generators.
- c) The geometrical moment of inertia at any section $a \sim f$ of the net is $I_n = 16 r^2 A_n$, A_n : sectional area of the generator, and that of the elevator shaft is I_s .
- d) The Z -component of direction cosines has the same value in every generator

$$e_z = \frac{h}{S} = 0.98, \quad S^2 = \left(\frac{a}{\sqrt{2}} + b \right)^2 + \left(\frac{a}{\sqrt{2}} \right)^2 + h^2, \quad S: \text{length of the generator.}$$

3. Stress Analysis (Lateral Force P at the Top of the Tower)

Both net and shaft may be regarded as jointed to the rigid body at the top and bottom of the tower, and relative displacement of the net and the shaft is restrained by diaphragms distributed at the nodes. So we may assume that the net and the shaft behave as a complete composite structure and that the applied moment is to be shared between the net and the shaft according to the ratio of the moments of inertia

$$M_n = \frac{1}{1+k} M, \quad M_s = \frac{k}{1+k} M, \quad k = \frac{I_s}{I_n}.$$

M : applied moment, M_n : moment acting on the net, M_s : moment acting on the shaft.

We divide the tower at two arbitrary adjacent node lines I.J. The shear force P and the bending moments $M_I = P h_1$, $M_J = P (h_1 + h_2)$ are then acting

on this portion of the shell (fig. 3). Deformations of an arbitrary point i of the section consist of the deformation due to shear δ_{x_0} and of the deformation due to bending δ_{z_i} ; these are also expressed by the meridional deformation δ_{m_i} and the hoop deformation δ_{θ_i} as shown in Fig. 4.

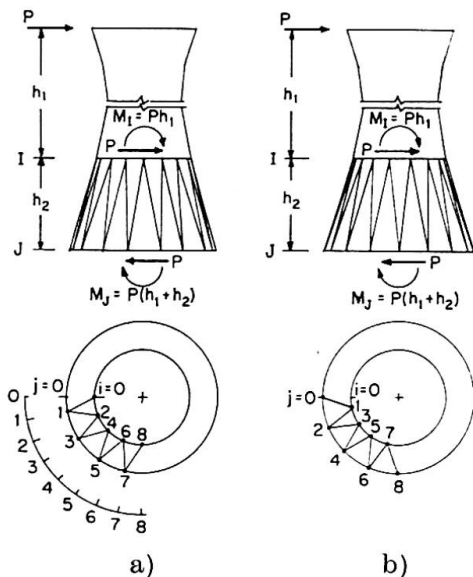


Fig. 3.

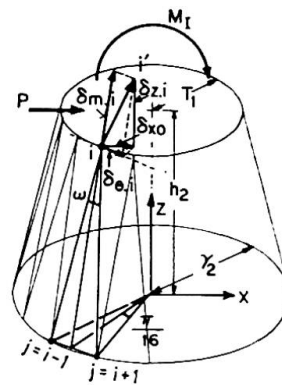


Fig. 4.

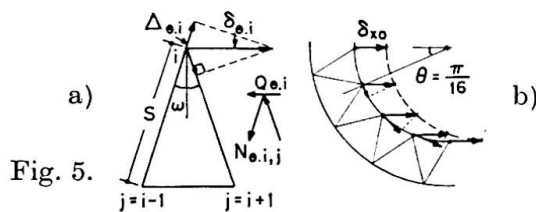


Fig. 5.

First, let us consider the stress due to deformation δ_{θ_i} . The axial deformation of the generator i, j is: $\Delta_{\theta_i} = \pm \delta_{\theta_i} \sin \omega$ (fig. 5 a), and the stress in it is

$$N_{\theta i, j} = \frac{\Delta_{\theta i}}{s} E A_n = \pm \frac{\delta_{\theta i}}{s} E A_n \sin \omega, \quad + \dots j = i - 1, \quad - \dots j = i + 1, \quad (3)$$

$$Q_{\theta, i} = (N_{\theta i, i-1} - N_{\theta i, i+1}) \sin \omega = \frac{2 \delta_{\theta i}}{s} E A_n \sin^2 \omega.$$

Let the shear deformation δ_{x_0} be same at any point i (fig. 5 b), and

$$\delta_{\theta i} = \delta_{x_0} \sin \frac{i \pi}{16}, \quad (4)$$

then
$$Q_{\theta i} = \frac{2 \delta_{x_0}}{s} E A_n \sin^2 \omega \sin \frac{i \pi}{16}.$$

The X-component of $\theta_{\theta i}$ is

$$Q_{\theta x i} = Q_{\theta i} \sin \frac{i \pi}{16} = \frac{2 \delta_{x_0}}{s} E A_n \sin^2 \omega \sin^2 \frac{i \pi}{16}. \quad (5)$$

Let us next consider the stress due to the deformation δ_{m_i} . The axial deformation of the generator Δ_{m_i} (fig. 6 a) is $\Delta_{m_i} = \delta_{m_i} \cos \omega$, and the stress in it is

$$N_{m i, j} = \frac{\Delta_{m i}}{s} E A_n = \frac{\delta_{m i}}{s} E A_n \cos \omega, \quad N_{m i, i-1} = N_{m i, i+1} = N_{m i}. \quad (6)$$

The resultant stress T_{mi} (fig. 6 a) is

$$T_{mi} = 2 N_{mi} \cos \omega = \frac{2 \delta_{mi}}{s} E A_n \cos^2 \omega.$$

The Z-component of T_{mi} is

$$T_{mzi} = T_{mi} \cos \phi = \frac{2 \delta_{mi}}{s} E A_n \cos^2 \omega \cos \phi. \tag{7}$$

In Fig. 6 b, we find the following relationships

$$S \cos \omega \cos \phi = h_2, \quad \therefore \cos \phi = \frac{h_2}{s \cos \omega} = \frac{e_z}{\cos \omega}, \tag{8}$$

$$r_2 \sin \frac{\pi}{16} = s \sin \omega, \quad \therefore \sin \omega = \frac{r_2}{s} \sin \frac{\pi}{16} = \frac{r_2}{h_2} e_z \sin \frac{\pi}{16}. \tag{9}$$

Introducing (8) into (7) we have

$$T_{mzi} = \frac{2 \delta_{mi}}{s} E A_n e_z \cos \omega. \tag{7'}$$

Z-component of deformation δ_{mi} is

$$\delta_{mzi} = \delta_{mi} \cos \phi = \delta_{mi} \frac{e_z}{\cos \omega}. \tag{10}$$

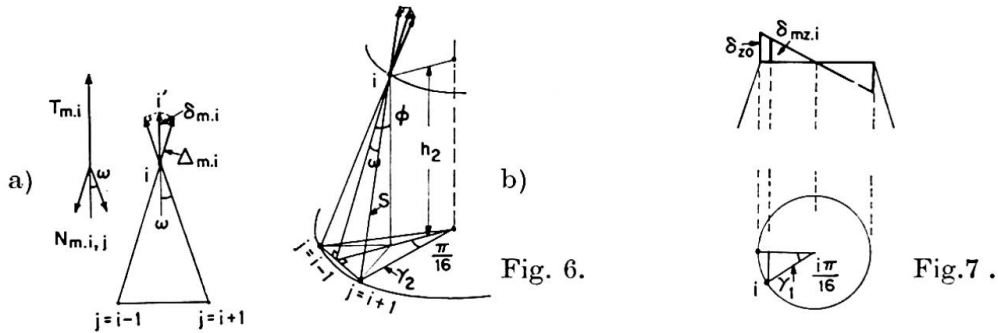


Fig. 6.

Fig. 7.

By introducing this value, (7) may also be written as follows:

$$T_{mzi} = \frac{2 \delta_{mzi}}{s} E A_n \cos^2 \omega. \tag{7''}$$

According to the assumption indicated at the beginning of this section, δ_{mzi} may be expressed as follows (fig. 7)

$$\delta_{mzi} = \delta_{z0} \cos \frac{i \pi}{16}. \tag{11}$$

And the moment at the point i is: $M_i = T_{mzi} r_1 \cos \frac{i \pi}{16}$.

Using (7) and (11): $M_i = \frac{2 \delta_{z0}}{s} E A_n r_1 \cos^2 \omega \cos^2 \frac{i \pi}{16}$.

Summing up at all the points of the section

$$\sum M_i = \frac{2 r_1}{s} E A_n \cos^2 \omega \delta_{z0} \sum \cos^2 \frac{i \pi}{16} = \frac{16 r_1}{s} E A_n \cos^2 \omega \delta_{z0}. \quad (12)$$

This must be equal to the applied moment

$$\frac{P h_1}{1 + k_1} = \frac{16 r_1}{s} E A_n \cos^2 \omega \delta_{z0}. \quad (13)$$

Introducing (13), (11) and (10) into (6), we obtain the stress of the generator due to the deformation δ_{mi}

$$N_{mi,j} = \frac{P h_1}{16 r_1 e_z (1 + k_1)} \cos \frac{i \pi}{16}. \quad (14)$$

Next, let us consider the X -component of stress T_{mi}

$$Q_{mxi} = \sum_j^{i-1, i+1} N_{mi,j} e_{xi,j} = N_{mi} (e_{xi, i-1} + e_{xi, i+1}), \quad (15)$$

where $e_{xi,j}$ is the X -component of direction cosines of the generator ij , and with reference to Fig. 3

$$e_{xi,j} = -\frac{r_1 \cos \frac{i \pi}{16} - r_2 \cos \frac{j \pi}{16}}{s}. \quad (16)$$

Introducing (14), (16) into (15) we have

$$Q_{mxi} = -\frac{P h_1}{8 h_2 (1 + k_1)} \left(1 - \frac{r_2}{r_1} \cos \frac{\pi}{16}\right) \cos^2 \frac{i \pi}{16}. \quad (17)$$

The resultant stress in the X -direction is

$$\begin{aligned} Q_{xi} = Q_{\theta xi} + Q_{mxi} &= \frac{2 \delta_{x0}}{s} E A_n \sin^2 \omega \sin^2 \frac{i \pi}{16} \\ &\quad - \frac{P h_1}{8 h_2 (1 + k_1)} \left(1 - \frac{r_2}{r_1} \cos \frac{\pi}{16}\right) \cos^2 \frac{i \pi}{16}. \end{aligned} \quad (18)$$

Summing up at all the points of the section

$$\begin{aligned} \sum Q_{xi} &= \frac{2 \delta_{x0}}{s} E A_n \sin^2 \omega \sum \sin^2 \frac{i \pi}{16} - \frac{P h_1}{8 h_2 (1 + k_1)} \left(1 - \frac{r_2}{r_1} \cos \frac{\pi}{16}\right) \sum \cos^2 \frac{i \pi}{16} \\ &= \frac{16 \delta_{x0}}{s} E A_n \sin^2 \omega - \frac{P h_1}{h_2 (1 + k_1)} \left(1 - \frac{r_2}{r_1} \cos \frac{\pi}{16}\right). \end{aligned} \quad (19)$$

Here we must consider the shear stress on the shaft

$$Q_s = \left\{ \frac{k_2}{1 + k_2} P (h_1 + h_2) - \frac{k_1}{1 + k_1} P h_1 \right\} \frac{1}{h_2} = \left\{ \frac{k_2}{1 + k_2} \left(1 + \frac{h_1}{h_2}\right) - \frac{k_1}{1 + k_1} \frac{h_1}{h_2} \right\} P. \quad (20)$$

The equilibrium between the stresses in the section and the applied force is

$$P = \sum Q_{xi} + Q_s. \quad (21)$$

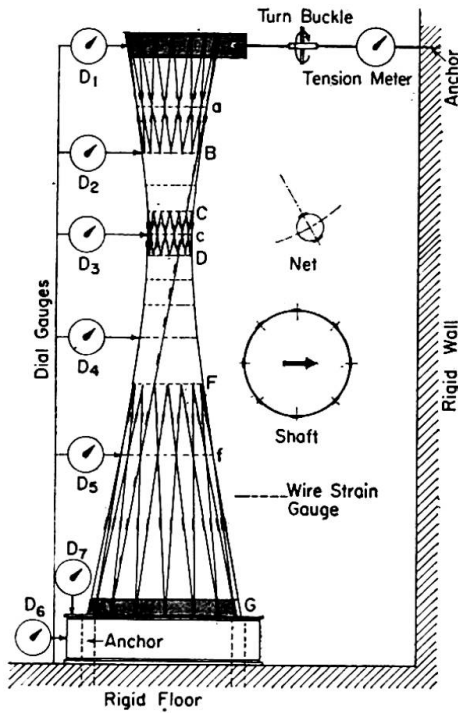


Fig. 8.

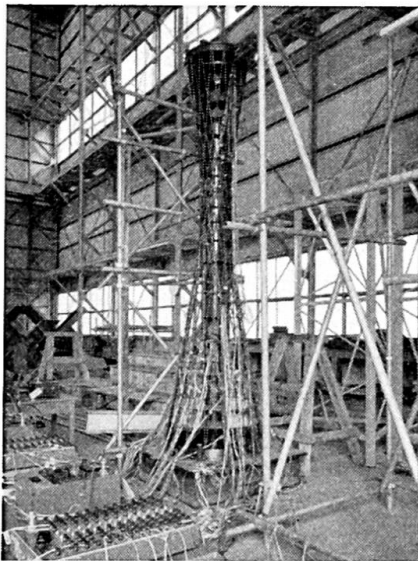


Fig. 10.

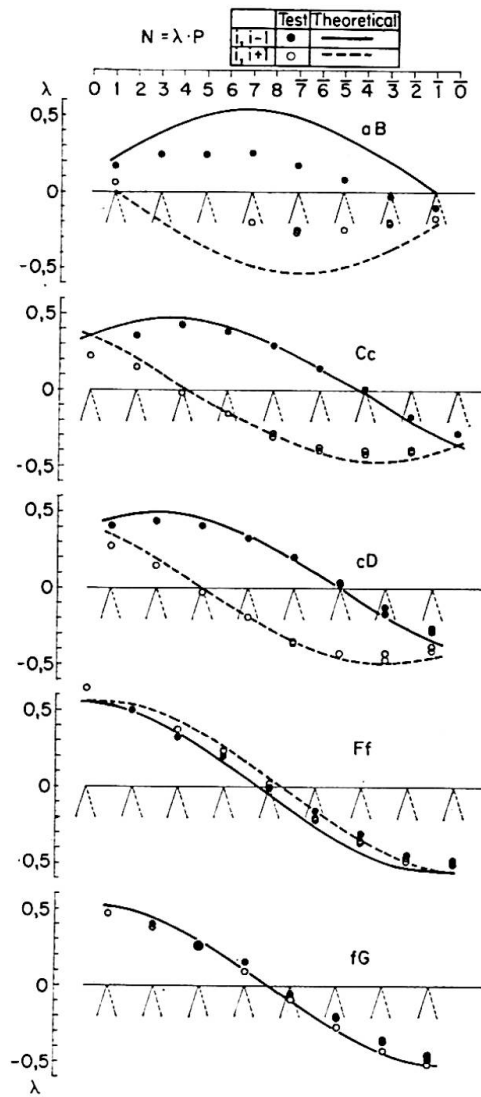


Fig. 9.

Introducing (19) and (20) into (21) we have

$$\delta_{x0} = \frac{s}{16 E A_n \sin^2 \omega} \left(\frac{1 + \alpha}{1 + k_2} - \frac{\alpha \beta}{1 + k_1} \cos \frac{\pi}{16} \right) \quad \text{where, } \alpha = \frac{h_1}{h_2}, \beta = \frac{r_2}{r_1}. \quad (22)$$

Introducing (4), (9) and (22) into (3) we have

$$N_{\theta i, j} = \pm \frac{P h_2}{16 r_2 e_z \sin \frac{\pi}{16}} \left(\frac{1 + \alpha}{1 + k_2} - \frac{\alpha \beta}{1 + k_1} \cos \frac{\pi}{16} \right) \sin \frac{i \pi}{16}, \quad (23)$$

$$+ \dots j = i - 1, \quad - \dots j = i + 1.$$

We now obtain the resultant stress of an arbitrary member ij

$$N_{i,j} = N_{m i,j} + N_{\theta i,j} = \frac{P}{16} \frac{h_2}{e_z r_2} \left\{ \frac{\alpha \beta}{1+k_1} \cos \frac{i\pi}{16} \pm \left(\frac{1+\alpha}{1+k_2} \operatorname{cosec} \frac{\pi}{16} - \frac{\alpha \beta}{1+k_1} \cot \frac{\pi}{16} \right) \sin \frac{i\pi}{16} \right\}, \quad (24)$$

$$+ \dots j = i-1, \quad - \dots j = i+1, \quad \alpha = \frac{h_1}{h_2}, \quad \beta = \frac{r_2}{r_1}, \quad k_1 = \frac{I_s}{8 r_1^2 A_n}, \quad k_2 = \frac{I_s}{8 r_2^2 A_n}.$$

4. Test Results

The test model has dimensions equal to $1/25$ of those of the actual tower as shown in Fig. 2, and each part of the model is made of steel.

A lateral force was applied at the top of the model by means of a tension bar, and the magnitude of the tensile force was measured by a tension meter inserted in the tension bar system as shown in Fig. 8. Seven dial gauges were used to measure the deflection of the model, and 360 electric resistance wire strain gauges were mounted to investigate the stress distribution of the model. The locations of the dial gauges and electric resistance wire strain gauges are shown in Fig. 8.

Some of the more important results are shown in Fig. 9, they are the stresses measured at all the main parts of the model. In Fig. 9, the theoretical values obtained by means of Eq. (24) are given in condition; the moment of inertia of the shaft I_s is 460 cm^4 in this model.

The calculated and the observed stresses show satisfactory agreement, except at the upper portion of the model aB . In Eq. (24), we have not considered the boundary effects at the top end of the model, and this might have affected the above results to some extent at the upper portion aB .

In the practical design of this tower, Eq. (24) was adopted as a design criterion, and some appropriate modification were therefore applied, for the upper portion of the tower by reference to the test results.

Summary

A unique tower as shown in Fig. 1 is now under construction on the 3rd pier of the port of Kobe. This tower consists of an outer net of one-sheet hyperboloid and the elevator shaft located in the core. This paper comprises the stress analysis and the experimental study of this tower when subjected to lateral forces such as the seismic load. The agreement between the test results and the theoretical results was satisfactory, and the method of calculation described would be adequate as a practical design criterion.

Résumé

Une tour d'un genre unique, visible à la fig. 1, est en cours de construction à la jetée n° 3 du port de *Kobé*. Cette tour comporte un treillis extérieur en hyperboloïde à une nappe et une cage d'ascenseur dans son noyau. L'auteur présente les résultats du calcul des contraintes et des recherches expérimentales effectuées sur cette tour soumise à des forces latérales telles que celles d'origine sismique. On constate un accord satisfaisant entre les essais et les résultats du calcul, et l'on en conclut que la méthode de calcul présentée devrait constituer un critère suffisant dans la pratique.

Zusammenfassung

Auf dem dritten Landungsdamm des Hafens von Kobe ist gegenwärtig ein einzigartiger Turm im Bau (siehe Abb. 1). Dieser Turm besteht aus einem äußeren Netzwerk in der Form eines einschaligen Hyperboloids und einem den Aufzug enthaltenden Kern. Die vorliegende Abhandlung beschreibt die Spannungsberechnung und die Modellmessungen unter der Wirkung seitlicher Kräfte insbesondere infolge von Erdbeben. Die Übereinstimmung der Versuchsergebnisse mit den rechnerischen Werten ist befriedigend, und die gewählte Berechnungsmethode darf für die Bedürfnisse der Praxis als ausreichend bezeichnet werden.